RESEARCH ARTICLE

The M_w 5.0 Kharsali, Garhwal Himalayan earthquake of 23 July 2007: source characterization and tectonic implications

Naresh Kumar*, Ajay Paul, A. K. Mahajan, D. K. Yadav and Chandan Bora

Wadia Institute of Himalayan Geology, 33 GMS Road, Dehradun 248 001, India

In the early morning hours of 23 July 2007 at 04 : 32 : 13.5 (IST), a moderate (M_L = 4.9, M_w = 5.0) earthquake occurred in the Garhwal Himalaya near Kharsali, about 50 km northwest of the epicentre of the strong (M 6.4) Uttarkashi earthquake of 20 October 1991. Sourced in the upper crust (15 km focal depth), this earthquake was followed by a series of shallow-focused aftershocks of magnitudes ≤ 3.4. Data from the local broadband seismic network were used for understanding the source characterization. The fault plane solutions of the main shock and the biggest aftershock (M 3.4) are almost similar, suggesting that the deformation occurred by reverse faulting with a significant strike–slip component. For the main shock, the trend/plunge of the major and minor principal axes P/T was 166°/1° and 258°/67° respectively. In these solutions one fault plane is dipping to the NE, and the strike of the fault plane coincides with the major tectonic faults as well as the longest axis of isoseismals. The seismic moment, source radius and stress drop of the main shock are estimated to be 4.15×10^{16} Nm, 1660 m and 4.15 MPa respectively.

Keywords: Fault plane, seismicity, source parameters, tectonic implications.

A MODERATE earthquake of magnitude M_L = 4.9 (M_w = 5.0) occurred in the Garhwal Himalaya on 23 July 2007 (22 July at 23 : 02 : 13.2 UTC) at 04 : 32 : 13.2 Indian Standard Time (IST), that was located near Kharsali at 15 km focal depth by local seismic network of the Wadia Institute of Himalayan Geology (WIHG), Dehradun, India. It was felt as far as Delhi (in the upper parts of a few multistorey buildings), located about 500 km from the epicentre (Figure 1). No casualty was reported; however, near the epicentre, a few adobe buildings suffered damage (grade 2–3) of intensity VI on the European Macroseismic Scale (EMS-98). WIHG deployed two additional portable seismographs near the main shock to record near-source, high-frequency ground motions for significant aftershock activities.

The Himalayan plate boundary has experienced several large earthquakes in the past and many moderate earthquakes have occurred in recent times[1]. A major earthquake (M_w 7.8) occurred in the Kashmir region[2,3] in 2005, killing about 80,000 people in Pakistan and India. Earlier, the Garhwal–Kumaon region in the Western Himalaya has been ruptured by two strong earthquakes (M 6.4 Uttarkashi 1991 and M 6.6 Chamoli 1999). The Garhwal–Kumaon region is seismologically important because it falls in the seismic gap of major earthquakes[4,5]. The earthquake catalogue of NW Himalaya compiled by WIHG[6] lists at least six major earthquakes during the last 400 years, indicating the large seismic potential of the Garhwal–Kumaon and surrounding regions (Figure 1). The Kharsali earthquake is the biggest event in the Garhwal–Kumaon region after the M 6.6 Chamoli earthquake of 1999 that occurred with two hidden source asperities[7].

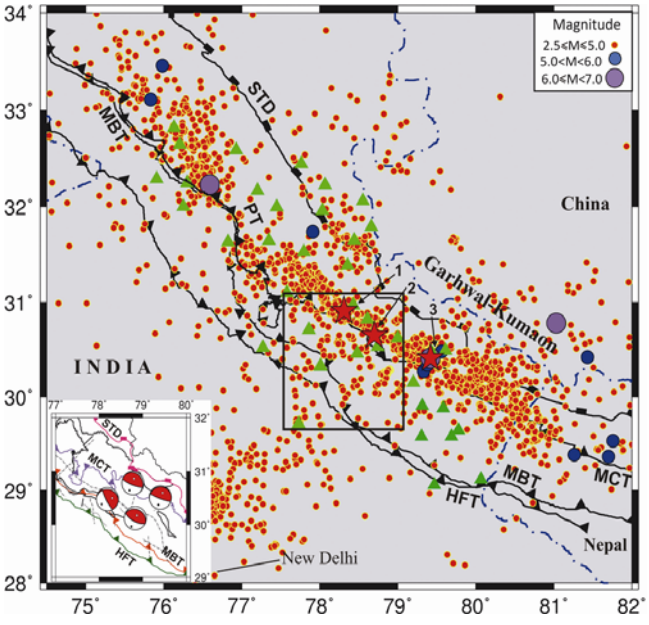

Figure 1. Seismotectonic map of NW Himalaya using seismicity ($M \geq 2.5$) for the period of 1999–2010. Purple circles are the strong earthquakes, the recent earthquakes of Garhwal–Kumaon with red circles are (1) M 4.9 Kharsali 2007, (2) M 6.4 Uttarkashi 1991 and (3) M 6.6 Chamoli 1999. The green triangles are stations and area marked by squares represents the present study region. STD, South Tibetan Detachment; MCT, Main Central Thrust; MBT, Main Boundary Thrust; PT, Panjal Thrust; HFT, Himalayan Frontal Thrust. (Inset) Fault plane solution (FPS) of past earthquakes.

*For correspondence. (e-mail: nkd@wihg.res.in)

The precursory signatures for this event were also observed in radon data[8].

Almost all the earthquakes of higher magnitude ($M \geq 5.5$) in the Himalaya have occurred at a depth of 15–20 km around the Main Central Thrust (MCT) in response to thrust tectonics[9] in the detachment zone along the northerly dipping Indian plate. It is described as the transition zone between the locked, shallow portions of the fault that rupture during great earthquakes and the smoothly sliding deeper aseismic zone[5]. It has also been observed that the earthquakes of smaller magnitude are mostly occurring at shallow depth above the detachment surface along the imbricate planes arising from the detachment zone around MCT[1,10]. The main shock of 23 July 2007 was triggered along one of the thrusting planes of MCT; however, it activated the asperity zone in the NE–SW direction at two places.

Instrumental analysis

The earthquake was recorded by several broadband and short-period seismic stations of the WIHG seismic network of NW Himalaya (green triangles, Figure 1). Twelve broadband seismic stations acquire data in continuous real mode at the central station, Dehradun, through VSAT telemetry network. The VSAT seismic network and some other standalone stations are equipped with broadband seismometers (Trillium 240) and high dynamic range Taurus digital data acquisition system. Other stations have broadband (CMG-3T and CMG-40T) and short-period (CMG-1T) seismometers connected with high dynamic range digitizers (REFTEK-130 and GURLAP). All stations collect data at 100 SPS. WIHG has also installed single vertical component seismic stations in the schools of NW Himalaya under the HIMSLEP programme, which are collecting data at 40 SPS.

The VSAT network data of 12 stations were sufficient to locate the Kharsali earthquake in the Garhwal Himalaya within a few minutes of its occurrence and later on the location was revised using a total of 40 stations (Figure 1). To obtain better azimuthal coverage of seismic stations from the northern side of the epicentre and to properly record aftershock activity, WIHG immediately installed two broadband portable seismic stations in the northern side at Ranachati and Mori. In the present work, the high-quality digital data were used to obtain both kinematic and dynamic source parameters.

Earthquake source locations

Using VSAT data of 12 stations, the Kharsali earthquake of 23 July 2007 was located within a few minutes of its occurrence using the HYPO71 program of the SEISAN software[11]. The main shock was also located by the United States Geological Survey (USGS) and India Meteorological Department (IMD), New Delhi. However, due to close proximity and good station azimuthal coverage, our location accuracy is much better compared to others. As given in Table 1, the error of initial source location in the horizontal direction is 4.5 km for the WIHG location and 12.6 km for USGS, whereas the error in vertical direction for the WIHG location is 9.5 km and USGS has given fixed focal depth of 35 km. Both agencies revised the source parameters using data of additional stations. Again, the WIHG network has higher accuracy (Table 1) highlighting the importance of the local network.

The revised WIHG location obtained using 35 P-phases and 31 S-phases with good station azimuthal coverage indicates horizontal error of only 2.5 km and vertical error of 4.5 km. The Vp/Vs ratio of 1.70 was obtained using the Wadati diagram for 20 S–P travel times (correlation coefficient of 0.998) showing an estimated origin time 23 : 02 : 13.22 (UTC). The revised USGS location had large modification in focal depth that changes from 35 km (initial estimate) to 14 km. The new focal depth of USGS was close to that of WIHG; however, the error was still higher (Table 1). The adoption of regional crustal velocity model (Table 2) by WIHG may also be one reason for less error because the crustal structure in the Himalaya is complex with high regional variability[10]. The main shock was followed by a sequence of aftershocks (Figure 2 *b*). We could obtain proper locations for only 35 aftershocks in the magnitude range $1.0 \leq M \leq 3.4$ (Table 3).

Tectonics and crustal velocity structure

The present study region is in the central part of NW Himalaya described as the MCT zone, where MCT has been divided into zones by the Vakrita Thrust (VT), Munsiari Thrust (MT) and Jutogh Thrust (JT) (Figure 2). These thrust sheets are northerly dipping lateral sequences, orogenically falling in the Lesser Himalaya (LH) and comprising fossiliferous Riphean sediments[12]. To its south is the Main Boundary Thrust (MBT), a northerly dipping thrust that separates LH from the Siwalik Himalaya (SH) and to the north of MCT (VT), the higher Himalaya consisting of the crystalline rocks (Figures 1 and 2). The mentioned thrusts dip steeply near the surface and flatten out at greater depth, merging with the detachment plane and hold the key to spatial disposition of earthquake occurrence[9].

Tectonically, the Himalaya is complex having variations in the crustal structures in the horizontal and vertical directions and the proper detection of earthquake sources is constrained by the limited work on the velocity models. Majority of earthquakes in the central Himalaya are shallow focus and source characterization would require finer crustal velocity models. Aftershock sequence of the M 6.6 Chamoli earthquake of 1999 was used[13] to

Table 1. Comparison of initial and revised source parameters of the main shock

	WIHG	USGS
Initial source parameters		
Date	22/07/2007	22/07/2007
Origin time	23 : 02 : 13.38 (UTC) Rms = 0.54 s	23 : 02 : 17.0 (UTC) Rms = 0.94 s
Epicentre	30.915N, 78.315E (± 4.5 km)	30.965N, 78.268E (± 12.6 km)
Depth	15.1 km (± 9.5 km)	35 km (fixed)
Magnitude	4.8 M_L	4.9 Mb
	Gap = 183°, Nst = 9	Gap = 122°, Nst = 29
Revised source parameters		
Date	22/07/2007	22/07/2007
Origin time	23 : 02 : 13.22 (UTC) Rms = 0.61s	23 : 02 : 14.35 (UTC) Rms = 0.94 s
Epicentre	30.910N, 78.316E (± 2.6 km)	30.938N, 78.275E (± 4.4 km)
Depth	15.0 km (± 4.9 km)	14 km (± 5.7 km)
Magnitude	4.9 M_L	5.0 Mb
	Gap = 97°, Nst = 40	

Table 2. 1D crustal model used taking S-wave velocities through *V*p/*V*s = 1.74 (1D model of Kangra–Chamba region[10])

Depth (km)	*V*p (km/s)
0.0	5.27
10.0	5.55
15.0	5.45
18.0	6.24
46.0	8.25

develop the four-layer 1D crustal model of Garhwal–Kumaon region, replacing the initial two-layer model[14]. Recently, a more refined four-layer crustal velocity model has been developed (Table 2) for the adjoining western Kangra–Chamba sector of NW Himalaya[10]. We tested all these models to locate the Kharsali earthquake and its aftershocks. We noticed that the obtained locations had the lowest error for the recent model[10].

Spectral source parameters and focal mechanism

The source model relates the corner frequency and low frequency asymptote to source dimension to obtain seismic moment[15]. Observations of spectra consistent with Brune's theory have been reported for large earthquakes[16] as well as microearthquakes[17] covering a wide range of earthquake source dimension. Detailed description of the theoretical approach and analysis of 18 events have been done earlier[7], where validation of source parameters was also performed using waveform modelling. Presently, 36 events have been analysed after computing P-wave displacement spectra to obtain corner frequency (f_c) and spectral amplitude (Ω_0). The spectral source parameters were computed using Brune's circular model with the following formulations[15,18]

$$Mo = 4\pi\rho v^3 D\Omega_0/R, \quad (1)$$

$$r = 2.34v/2\pi f_c, \quad (2)$$

$$\Delta\sigma = 7Mo/16r^3, \quad (3)$$

where Mo, r, $\Delta\sigma$, ρ, v, D and R denote seismic moment (Nm), source radius (m), stress drop (MPa), density (kg/m^3), velocity (m/s), hypocentral distance (km) and radiation pattern respectively. The obtained seismic moment, source radius and stress drop had values 4.15×10^{16} Nm, 1660 m and 4.15 MPa respectively, resulting in a moment magnitude of 5.0 for the main shock. These parameters were also obtained for 35 aftershocks (Table 4), indicating variations of 1.7×10^{13} to 8.0×10^{14} Nm, 350 to 670 m and 0.01 to 2.0 MPa for seismic moment, source radius and stress drop respectively. The low stress drop is close to the specified range of the inter-plate region of the Himalaya. However, its large variation (0.01–4.15 MPa) violates the concept of constant stress drop for one region[18]. The focal mechanism of the main shock provides evidence of subsurface tectonic deformation in the hypocenteral zone. Past solutions mostly of intermediate and larger-sized earthquakes in the Himalayan region indicate dominance of thrust-faulting[9,19] that also prevailed in the present region[1] (inset, Figure 1). However, the composite focal mechanisms based on smaller-sized earthquakes in the present study region have a variable trend with pure thrust mechanism in the eastern part of the Bhagirathi valley and strike–slip solutions in the western part along the Yamuna valley[14,20,21].

Using polarities of P-wave first motion at more than 20 stations, the fault plane solutions (FPSs) of the Kharsali earthquake and its biggest aftershock (M 3.4) were obtained using a reasonable maximum station azimuthal gap of 97° and 142° respectively. The program FOCMEC was used to search for the parameter space of possible double-couple orientations using appropriate filters for

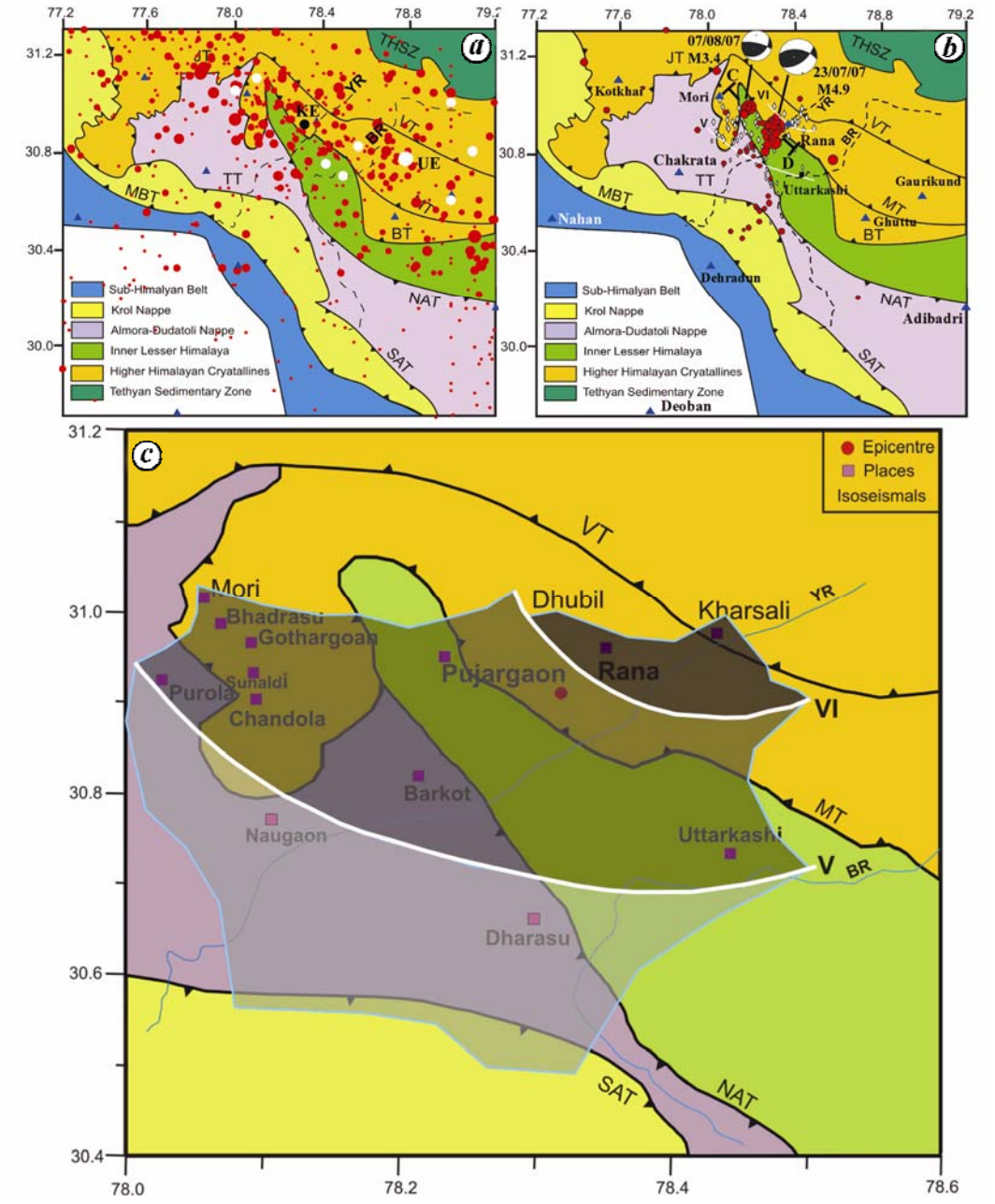

Figure 2. ***a***, Past seismicity (1965–2005) of the present region along with regional tectonics[6]. KE, Kharsali earthquake (2007); UE, Uttarkashi earthquake (1991). ***b***, *M* 4.9 Kharsali earthquake and its aftershocks are shown with red circles. Broadband stations are shown with blue triangles and the intensities evaluated at different places with white rhombus, CD is the profile referred to in Figure 4. ***c***, Isoseismal zones of intensities VI, V and IV (shaded areas) are well constrained based on data at approximately 70 sites. White curves are isoseismals (V and VI) shown with open-ended contours.

broadband data[22]. Two nodal planes were identified after denoting compressive motion with filled circles and dilatation through open circles (Figure 3). Both the solutions (Table 5; Figure 3) show oblique movement on a reverse fault with significant strike–slip component. In both cases, one fault plane is dipping toward NE coinciding with the dipping Himalayan thrust sheets, whereas the other plane is dipping toward SE. Both the nodal planes of the main shock are dipping with almost same angle of 48.54° and 50.25° towards NE and SE respectively, whereas the aftershock located towards NW at shallow focal depth has a steep dip of 71.5° for the NE-dipping plane and a gentle dip of 28° for the SE-dipping plane. The trend/plunge for the main shock of the *P*- and *T*-axis is 166°/1° and 258°/67° respectively. The NE-dipping plane was considered as the nodal plane because the dipping of the major tectonics of the region matches with it and also the dip angles (steep for shallow focus and gentle for deep focus) agree with the general conceptual model of the Himalaya[9]. It indicates the listric form of

Table 3. Obtained source parameters of the Kharsali earthquake and aftershocks

Date (YY-MM-DD)	Time (HR : MIN : SEC)	Latitude (°N)	Longitude (°E)	Depth (km)	M_L
2007-07-22	23 : 02 : 13.2	30.911	78.317	15.0	4.9
2007-07-22	23 : 05 : 53.9	30.837	78.313	8.3	3.1
2007-07-22	23 : 07 : 50.7	30.924	78.309	10.0	2.2
2007-07-22	23 : 09 : 24.5	30.897	78.323	18.0	2.0
2007-07-22	23 : 12 : 08.6	30.910	78.316	10.0	1.9
2007-07-22	23 : 12 : 50.4	30.950	78.297	10.0	1.8
2007-07-22	23 : 18 : 45.4	30.919	78.238	4.9	1.0
2007-07-22	23 : 25 : 16.1	30.880	78.321	23.3	1.5
2007-07-22	23 : 38 : 53.8	30.830	78.280	13.6	1.9
2007-07-22	23 : 45 : 07.0	30.863	78.307	14.3	1.6
2007-07-22	23 : 57 : 53.5	30.910	78.313	10.1	1.5
2007-07-23	05 : 39 : 17.0	30.898	78.323	12.0	2.1
2007-07-23	06 : 33 : 20.8	30.890	78.271	15.1	2.2
2007-07-23	07 : 57 : 05.4	30.919	78.304	15.1	2.2
2007-07-23	08 : 00 : 00.3	30.888	78.300	24.3	1.2
2007-07-23	09 : 08 : 08.1	30.912	78.308	15.1	2.3
2007-07-23	20 : 19 : 59.5	30.853	78.268	15.1	1.2
2007-07-25	07 : 25 : 28.2	30.937	78.322	13.3	1.5
2007-07-28	15 : 05 : 13.2	30.883	78.266	15.1	1.6
2007-07-29	23 : 47 : 13.0	30.801	78.269	21.5	1.8
2007-08-03	23 : 49 : 22.6	30.876	78.321	12.7	1.6
2007-08-04	12 : 21 : 16.0	30.913	78.277	13.0	1.6
2007-08-06	16 : 48 : 34.6	30.927	78.319	13.0	1.5
2007-08-07	10 : 11 : 40.2	30.986	78.194	6.5	3.4
2007-08-07	10 : 32 : 46.4	30.959	78.173	6.6	2.0
2007-08-07	12 : 27 : 49.8	30.973	78.174	4.7	1.5
2007-08-07	13 : 11 : 24.7	30.986	78.169	0.0	1.3
2007-08-07	14 : 39 : 00.5	30.964	78.159	0.0	1.0
2007-08-07	15 : 56 : 22.3	30.920	78.257	8.3	1.2
2007-08-09	05 : 27 : 23.6	30.990	78.195	12.6	1.2
2007-08-09	09 : 35 : 24.7	30.947	78.324	17.8	1.5
2007-08-09	10 : 41 : 12.4	30.956	78.171	5.0	1.7
2007-08-10	12 : 45 : 56.7	30.909	78.286	14.5	1.4
2007-08-17	20 : 12 : 09.2	30.948	78.175	0.0	1.2
2007-08-18	12 : 28 : 56.4	30.980	78.177	0.0	1.4
2007-08-19	02 : 35 : 12.1	30.954	78.161	7.5	1.0

major tectonic faults, i.e. MCT in this case, that has higher dip angle at shallow depth which goes on decreasing in deeper section and ultimately merging with the detachment plane in the mid-crust.

Considering the complex geotectonics and consistency in observations, the aftershock activity in the vicinity of the main shock in the depth range of 5–15 km was utilized to obtain composite FPS. The result of composite FPS suggests pure strike–slip movement indicating tear-fault deformation. The strike–slip movement is in agreement with previous FPS of the Yamuna valley region[14,20,21]. The aftershock activity near the main shock and the strike–slip mechanism are correlated with the Yamuna tear fault[23].

Isoseismal studies

The area affected by the earthquake has been surveyed for assessment of intensity around the epicentral zone of the main shock on EMS scale as adopted earlier[3] in the NW Himalayan region during the *M* 7.6 Kashmir earthquake of 8 October 2005. The survey was started from Dehradun town (about 80 km towards south of the epicentre, Figure 2), where the earthquake was felt by many people while sleeping but no cracks were noticed in the buildings. We followed the Dehradun–Purola–Mori traverse moving towards the epicentre from the western side. At Khursoon village, about 30 km SE from Purola, development of a small minor hair-crack was noticed in the adobe house. The intensity was observed to increase while proceeding towards the epicentre and intensity V was assigned to the Purola region. The Purola Tehsil has a number of small villages; some are situated on hard bedrocks and some on alluvial deposits along the river bed. The villages situated on the river bed suffered cracks in most of the houses, varying from minor hair-cracks (grade-1) in concrete buildings (class 'C') to grade-2 damage in adobe houses. Gothatgaon village suffered a

higher damage of grade-2. Further north, at Mori the damage was less due to safe construction of houses (mostly wooden structure), although people were frightened and rushed outside. Due to shifting of furniture, swinging of hanging objects, etc., the region was assigned intensity V+. On the way to Yamnotri, small villages like Rana, Dubli, Nishni, Pirakemesh, Klipa, Dangroo and Pindki showed maximum damage that varied from grade-2 to grade-4 (partial collapse) in adobe houses, although most dwellings are situated on hard rocks. This area was assigned intensity VI and considered as a meizoseismal zone. Further east, the damage was noticed decreasing towards Drashu (Uttarkashi). The important observation was the transverse swinging of objects at Purola, Mori and Gothatgaon compared to up-down motion in the miezoseismal zone (Rana, Dubli, Nishni, etc.) as reported by the residents. Thus, the damage pattern indicates oblate shaped isoseismals (Figure 2 *c*) with longer axis towards NNW–SSE, and maximum damage was noticed in the western side due to inhabitation on the river bed.

Table 4. Obtained spectral source parameters using Brune's circular mode[15]

Seismic moment, *Mo* (Nm)	Source radius, *r* (m)	Stress drop, $\Delta\sigma$ (MPa)
4.15 × 10e16	1660	4.150
6.60 × 10e14	540	1.830
2.20 × 10e14	673	0.320
2.90 × 10e14	474	1.220
2.40 × 10e14	510	0.790
3.20 × 10e14	492	0.980
1.50 × 10e14	596	0.310
2.20 × 10e13	465	0.100
6.60 × 10e13	588	0.150
8.00 × 10e14	494	0.970
2.30 × 10e14	352	0.760
1.70 × 10e14	460	0.600
7.60 × 10e13	381	1.070
2.40 × 10e14	459	0.350
6.50 × 10e13	430	0.250
7.12 × 10e13	501	0.100
1.70 × 10e13	434	0.700
7.50 × 10e13	366	0.860
8.08 × 10e12	694	0.010
6.17 × 10e11	494	0.008
6.65 × 10e11	451	0.003
6.63 × 10e12	469	0.028
2.85 × 10e11	352	0.010
3.32 × 10e13	404	0.220
2.37 × 10e12	415	0.017
3.32 × 10e11	400	0.002
2.37 × 10e11	397	0.003
1.87 × 10e11	348	0.010
2.76 × 10e12	414	0.009
4.70 × 10e10	394	0.005
1.42 × 10e11	540	0.008
2.37 × 10e12	438	0.080
3.30 × 10e11	340	0.010
2.46 × 10e11	423	0.020
3.30 × 10e11	422	0.010
1.42 × 10e11	540	0.008

Table 5. Fault plane solution of *M* 4.9 and *M* 3.4 obtained using the first polarity motion

Nodal plane	Strike	Dip	Rake
M 4.9			
I	277.46	48.54	121.43
II	54.93	50.25	59.46
M 3.4			
I	282.72	71.5	111.17
II	52.41	27.99	43.22

Discussion and conclusion

The Garhwal Himalaya is seismically active and typically known for inter-plate seismic zone of thrust tectonic regime[1,14,20,21]. The seismicity shows NW–SE (Figures 1 and 2 *a*) trend around the surface trace of MCT. The spatio-temporal distribution of earthquakes in the NW Himalaya (Figure 1) indicates a large gap of major earthquakes in the Garhwal–Kumaon region. However, the last two decades have witnessed two strong earthquakes (i.e. 1991 Uttarkashi and 1999 Chamoli), which were located SE of the Kharsali earthquake. The epicentre of the Kharsali earthquake (Figure 2 *b*) is close to MT in the western side of the Yamuna valley.

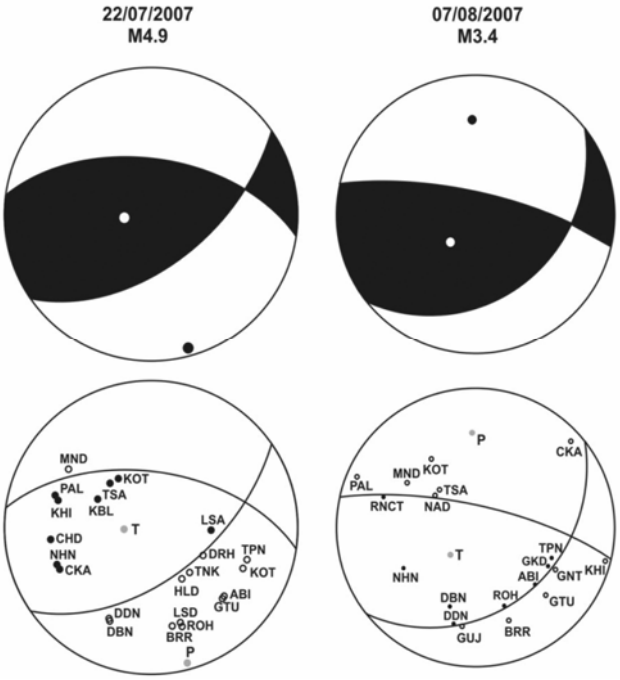

Figure 3. FPS equal area projection of the lower hemisphere. Positive and negative first polarity motions at different stations are shown with filled and open circles respectively, along with station codes. *P* and *T* mark the direction of maximum compression and extension axes.

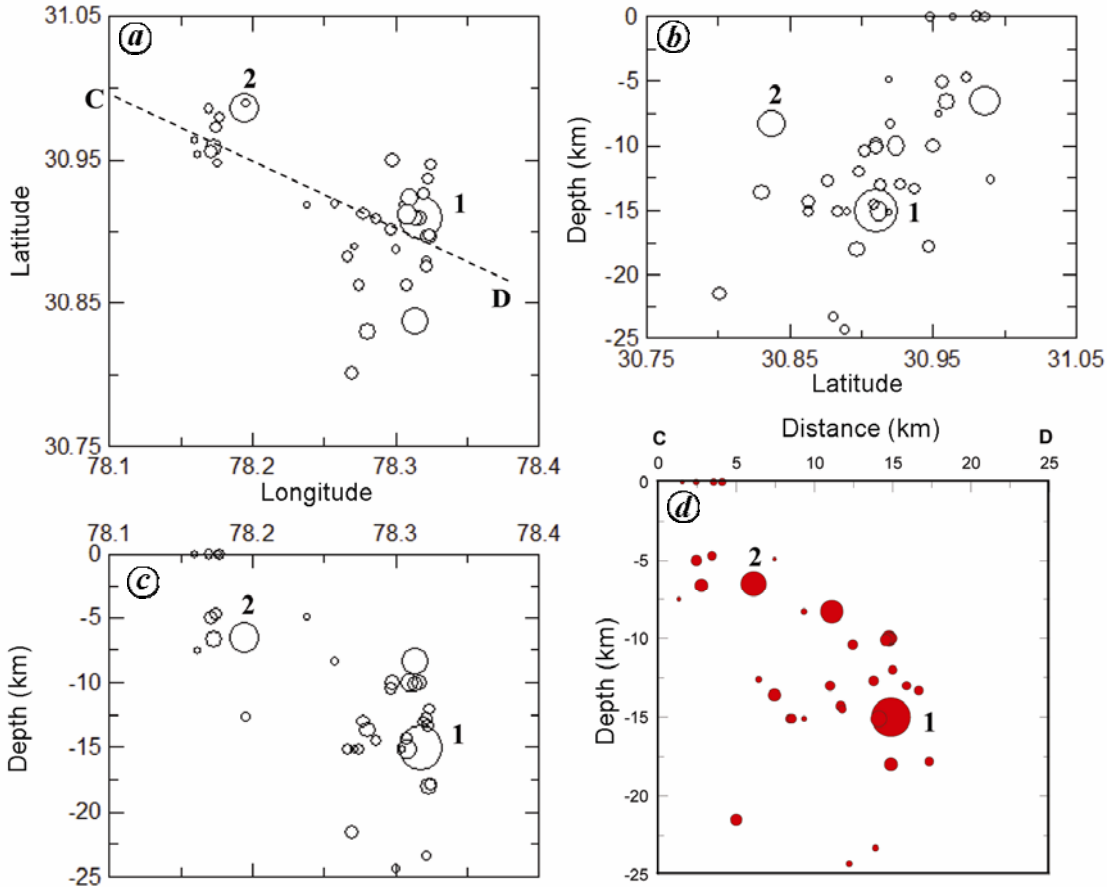

Figure 4. Locations of the main shock and well-located aftershocks (1: M_w 5.0 and 2: M 3.4). ***a***, Epicentre plot showing two clusters and cross-section CD. ***b***, Hypocentres along latitude. ***c***, Hypocentres along longitude. ***d***, Depth section plot of the events along cross-section CD.

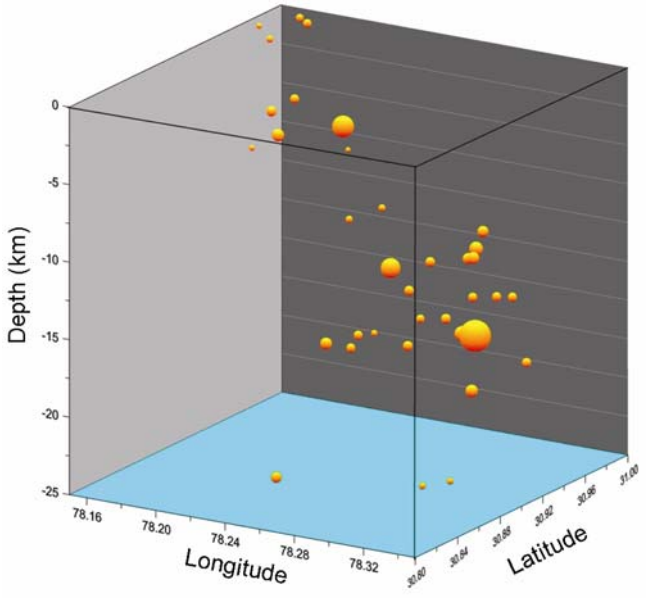

Figure 5. Three-dimensional bubble plot of the main shock and well-located aftershocks. The increasing size of the bubble corresponds to increasing magnitude of the earthquakes. Clusters around the main shock and large-sized aftershocks are visible at two different depth sections.

Within a period of one month, after the occurrence of the Kharsali earthquake, a total of 66 aftershocks were recorded by the WIHG network and hypocentres of 35 ($1.0 \leq M \leq 3.4$) of these events were well located using reasonable station azimuthal coverage (Table 3). In Figure 4, the epicentres and hypocentres are plotted along longitude, latitude and cross-section CD, indicating two clusters of aftershock activity. Initially, the aftershocks were concentrated close to the main shock (bigger cluster), whereas after 15 days on 7 August an M 3.4 event occurred in the northwest side that was followed by few smaller-sized earthquakes that make a new cluster. Almost all the aftershocks were located at shallow depths above the main shock, which is generally observed in the regions having high seismicity in the upper crust. The dense local network of WIHG and the refined regional velocity model[10] helped us to evaluate the earthquake data of the M_w 5.0 Kharsali earthquake and its aftershocks in the context of the seismotectonics of the Garhwal Himalaya. The 3D bubble plot of the hypocentres suggests northwest to southeast-dipping plane (Figure 5). The epicentres of these events also show a gap between the two clusters while moving from NW to SE along

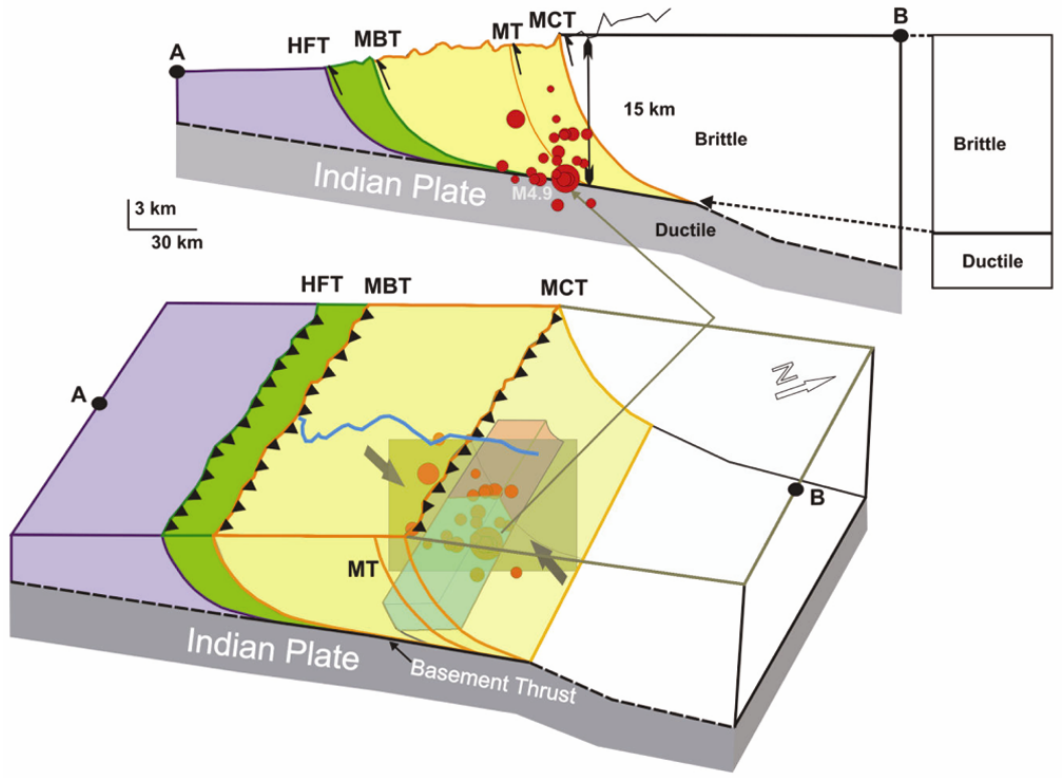

Figure 6. Seismotectonic model obtained through earthquake source locations and two recent FPS. Arrows indicate deformation during the main shock that occurred at the basement thrust where Munsiari Thrust (MT) originated. Two blocks (cyan and pink) separated by the Yamuna tear fault (shown by a rectangle that coincides with the Yamuna river – blue colour line) indicate the displacement that occurred during the Kharsali earthquake. Observed aftershock activity seems to be aligned along the Yamuna tear fault.

profile CD. The occurrence of relatively larger magnitude aftershock after 15 days which occurred on 7 August was followed by a few more events of smaller size, which suggests the NW migration of the activity.

The important observation is that the main shock as well as the aftershocks occurred to the south of MCT, where the local tectonic fault (MT) originated (Figure 2). In this region, it was also observed that the seismic activity during Uttarkashi (1991) and Chamoli (1999) earthquake occurred to the south of MCT[24]. Therefore, the potential active fault segments in the Garhwal Himalaya are to the south of MCT, where moderate-sized earthquakes occur in the upper crust above the basement thrust. The trend of the aftershocks at the shallow depth close to the main shock is not parallel to the NNW–SSE trend of the isoseismals V and VI. The composite fault plane solution of aftershocks (5–15 km depth) shows a dominant strike–slip mechanism coinciding with the Yamuna tear fault. This type of tectonic deformation for the aftershock activity is possible in the complex tectonic structure of the Garhwal Himalaya, as has also been reported earlier[24].

The calculated 48° dip of the main shock FPS is on the higher side compared to most of the previous Himalayan earthquakes at that focal depth[9]. However, steeply dipping fault planes of a few individual earthquakes[9,19] and of composite FPSs[14,20,21] were also reported earlier in the Garhwal–Kumaon Himalaya, which are considered to be associated with duplexes[25]. The validation of the seismotectonic model (Figure 6) and the prevailing thrusting mechanisms in the Himalaya support the NE-dipping plane as the nodal plane of both FPSs on the following basis.

1. The NE-dipping plane is in agreement with major tectonics of the Garhwal Himalaya.
2. The main shock has relatively smaller dip (48°) in the deeper part compared to a steep dip (71°) of shallow focus aftershock favouring the listric fault mechanism of the Himalaya.
3. For the main shock, the deformation occurred along the basement thrust dipping NE, whereas in the upper strata (only aftershocks close to the main shock), the deformation supports rupturing parallel to the Yamuna tear fault.

Based on the above inferences the seismotectonic model for the Kharsali earthquake is given in Figure 6. The geometry of the basement plane dipping towards NE is incorporated from the previous studies of that region[1,26]

as a part of the upper crust[10]. The section of this plane close to the focus of the main shock is further constrained by 15 km focal depth obtained through the present WIHG data. Probably the rupture during main shock occurred at the junction of the basement plane and MT.

Due to inaccessibility and poor inhabitation in the northern part, we could not properly study the macroseismic intensity. We were able to incorporate the isoseismal lines of only intensities V and VI putting open-ended towards northern side (Figure 2 *b* and *c*). The instrumental epicentre is close to the maximum intensity.

1. Kayal, J. R., Microearthquake activity in some parts of the Himalaya and the tectonic model. *Tectonophysics*, 2001, **339**, 331–351.
2. Rao, N. P., Kumar, P., Kalpna, Tsukuda, T. and Ramesh, D. S., The devastating Muzaffarabad earthquake of 8 October 2005: new insights into Himalayan seismicity and tectonics. *Gondwana Res.*, 2006, **9**, 365–378.
3. Mahajan, A. K., Kumar, N. and Arora, B. R., Quick look isoseismal map of 8 October 2005 Kashmir earthquake. *Curr. Sci.*, 2006, **91**, 356–361.
4. Khattri, K. N. and Tyagi, A. K., Seismicity patterns in the Himalayan plate boundary and identification of the areas of high seismic potential. *Tectonophysics*, 1983, **96**, 281–297.
5. Bilham, R., Gaur, V. K. and Molnar, P., Himalayan seismic hazard. *Science*, 2001, **293**, 1442–1444.
6. Lyubushin, A. A., Arora, B. R. and Kumar, N., Investigation of seismicity in western Himalaya. *Russ. J. Geophys. Res*., 2010, **11**, 27–34.
7. Paul, A. and Kumar, N., Estimates of source parameters of *M* 4.9 Kharsali earthquake using waveform modelling. *J. Earth Syst. Sci*., 2010, **119**, 731–743.
8. Choubey, V. M., Kumar, N. and Arora, B. R., Precursory signatures in the radon and geohydrological borehole data for *M* 4.9 Kharsali earthquake of Garhwal Himalaya. *Sci. Total Environ*., 2010, **407**, 5877–5883.
9. Ni, J. F. and Barazangi, M., Seismotectonics of the Himalayan collision zone: geometry of the underthrusting Indian plate beneath the Himalaya. *J. Geophys. Res*., 1984, **89**, 1147–1163.
10. Kumar, N., Sharma, J., Arora, B. R. and Mukhopadhyay, S., Seismotectonic model of the Kangra–Chamba sector of NW Himalaya: constraints from joint hypocenter determination and focal mechanism. *Bull. Seismol. Soc. Am*., 2009, **99**, 95–109.
11. Havskov, J. and Ottemoller, L., SEISAN earthquake analysis software. *Seismol. Res. Lett.*, 2000, **70**, 532–534.
12. Valdiya, K. S., *Geology of the Kumaon Lesser Himalaya*, Wadia Institute of Himalayan Geology, Dehradun, 1980, p. 291.
13. Mukhopadhyay, S. and Kayal, J. R., Seismic tomography structure of the 1999 Chamoli earthquake source area in the Garhwal Himalaya. *Bull. Seismol. Soc. Am*., 2003, **93**, 1854–1861.
14. Khattri, K. N., Chander, R., Gaur, V. K., Sarkar, I. and Kumar, S., New seismological results on the tectonincs of the Garhwal Himalaya. *Proc. Indian Acad. Sci*., 1989, **98**, 91–109.
15. Brune, J. N., Tectonic stress and the spectra of seismic shear waves from earthquakes. *J. Geophys. Res*., 1970, **75**, 4997–5009.
16. Hanks, T. C. and Wyss, M., The use of body wave spectra in the determination of seismic source parameters. *Bull. Seismol. Soc. Am*., 1972, **62**, 561–589.
17. Kumar, B. A., Ramana, D. V., Kumar, C. P., Rani, V. S., Shekhar M., Srinagesh, D. and Chadha, R. K., Estimation of source parameters for 14 March 2005 earthquake of Koyna–Warna region. *Curr. Sci*., 2006, **91**, 526–530.
18. Sharma, M. L. and Wason, H. R., Occurrence of low stress drop earthquake in the Garhwal Himalaya region. *Phys. Earth Planet. Inter*., 1994, **85**, 265–272.
19. Branowski, J., Armburster, J., Seeber, L. and Molnar, P., Focal depths and fault plane solutions of earthquakes and active tectonics of the Himalaya. *J. Geophys. Res*., 1984, **89**, 6918–6928.
20. Gaur, V. K., Chander, R., Sarkar, I., Khattri, K. N. and Sinvhal, H., Seismicity and the state of stress from investigations of local earthquakes in the Kumaon Himalaya. *Tectonophysics*, 1984, **118**, 243–251.
21. Sarkar, I., Chander, R., Khattri, K. N. and Sharma, P. K., Evidence from small magnitude earthquakes on the active tectonics of Northwest Garhwal Himalaya. *J. Himalayan Geol*., 1993, **4**, 279–284.
22. Snoke, J. A., Munsey, J. W., Teague, A. C. and Bollinger, G. A., A program for focal mechanism determination by combined use of polarity and SV-P amplitude ratio data. *Earthquake Notes*, 1984, **55**, 15.
23. Sahoo, P. K., Kumar, S. and Singh, R. P., Neotectonic study of Ganga and Yamuna tear faults, NW Himalaya, using remote sensing and GIS. *Int. J. Remote Sensing*, 2000, **21**, 499–518.
24. Kayal, J. R., Ram, S., Singh, O. P., Chakraborty, P. K. and Krunakar, G., Aftershocks of the March 1999 Chamoli earthquake and seismotectonic structure of the Garhwal Himalaya. *Bull. Seismol. Soc. Am*., 2003, **93**, 109–117.
25. Srivastava, P. and Mitra, G., Thrust geometries and deep structure of the outer and lesser Himalaya, Kumaon and Garhwal (India): implications for evolution of Himalayan fold-and-thrust belt. *Tectonics*, 1994, **13**, 89–109.
26. Prasad, B. R., Klemperer, S. L., Rao, V. V., Tewari, H. C. and Khare, P., Crustal structure beneath the sub-Himalayan fold-thrust belt, Kangra recess, northwest India, from seismic reflection profiling: implications for Late Paleoproterozoic orogenesis and modern earthquake hazard. *Earth Planet. Sci. Lett.*, 2011, **308**, 218–228.

ACKNOWLEDGEMENTS. We thank the Director, WIHG, Dehradun for permission to publish this paper, and also Prof. B. R. Arora and Dr V. M. Choubey for valuable suggestions. The Ministry of Earth Science, Government of India is acknowledged for providing funds through a project (MoES/P.O. (Seismo)/GPS/60/2006). N.K. thanks ICTP, Trieste, Italy for providing Junior Associateship. We also thank the reviewers for their comments that helped to improve the manuscript.

Received 16 May 2011; revised accepted 1 May 2012